Imaging Science in Dentistry 2022; 52: 267-73
https://doi.org/10.5624/isd.20220040

Influence of kilovoltage- peak and the metal artifact reduction tool in cone-beam computed tomography on the detection of bone defects around titanium-zirconia and zirconia implants

Rocharles Cavalcante Fontenele[1,*], Eduarda Helena Leandro Nascimento[2], Ana Catarina Imbelloni-Vasconcelos[3], Luciano Augusto Cano Martins[1], Andrea dos Anjos Pontual[3], Flávia Maria Moraes Ramos-Perez[3], Deborah Queiroz Freitas[1]

[1]*Department of Oral Diagnosis, Division of Oral Radiology, Piracicaba Dental School, University of Campinas, Piracicaba, SP, Brazil*
[2]*Department of Dentistry, Division of Oral Radiology, Odontomed Imagem - Medical and Dental Services, Recife, PE, Brazil*
[3]*Department of Clinical and Preventive Dentistry, Division of Oral Radiology, Federal University of Pernambuco, Recife, PE, Brazil*

ABSTRACT

Purpose: The aim of this study was to assess the influence of kilovoltage- peak (kVp) and the metal artifact reduction (MAR) tool on the detection of buccal and lingual peri-implant dehiscence in the presence of titanium-zirconia (Ti-Zr) and zirconia (Zr) implants in cone-beam computed tomography (CBCT) images.

Materials and Methods: Twenty implant sites were created in the posterior region of human mandibles, including control sites (without dehiscence) and experimental sites (with dehiscence). Individually, a Ti-Zr or Zr implant was placed in each implant site. CBCT scans were performed using a Picasso Trio device, with variation in the kVp setting (70 or 90 kVp) and whether the MAR tool was used. Three oral radiologists scored the detection of dehiscence using a 5-point scale. The area under the receiver operating characteristic (ROC) curve, sensitivity, and specificity were calculated and compared by multi-way analysis of variance ($\alpha = 0.05$).

Results: The kVp, cortical plate involved (buccal or lingual cortices), and MAR did not influence any diagnostic values ($P > 0.05$). The material of the implant did not influence the ROC curve values ($P > 0.05$). In contrast, the sensitivity and specificity were statistically significantly influenced by the implant material ($P < 0.05$) with Zr implants showing higher sensitivity values and lower specificity values than Ti-Zr implants.

Conclusion: The detection of peri-implant dehiscence was not influenced by kVp, use of the MAR tool, or the cortical plate. Greater sensitivity and lower specificity were shown for the detection of peri-implant dehiscence in the presence of a Zr implant. ***(Imaging Sci Dent 2022; 52: 267-73)***

KEY WORDS: Peri-Implantitis; Cone-Beam Computed Tomography; Dental Implants; Zirconium; Titanium

Introduction

The success of oral rehabilitation of partially or totally edentulous patients by titanium dental implant placement is well established in the literature.[1,2] However, patients with a thinner mucosal biotype may present negative aesthetic results, given the gray color of this type of implant material. In these cases, zirconia (Zr) dental implants are advantageous, advantages, as Zr is a metal-free, ceramic material that is biocompatible and has high resistance to flexion and hardness.[3] Regardless of the type of implant material, implants are susceptible to bone loss, and bone loss affecting the alveolar process around an implant at the cervical level is known as peri-implant dehiscence.[3] Several factors may influence the development of this inflammatory clinical condition, such as the thinness or thickness of bone and gingival tissues, accumulation of inflammatory biofilm, unfavorable anatomical conditions, inadequate implant placement, and an excessive load.[1,4,5]

The early diagnosis of peri-implant bone defects is one

This study was financed in part by the Coordenação de Aperfeiçoamento de Pessoal de Nível Superior - Brasil (CAPES) - Finance Code 001.
Received February 26, 2022; Revised May 7, 2022; Accepted May 24, 2022
Published online July 5, 2022
*Correspondence to : Prof. Rocharles Cavalcante Fontenele
University of Campinas, Piracicaba Dental School, Department of Oral Diagnosis, Av. Limeira, 901, Zip Code 13414-903, Piracicaba, Sao Paulo, Brazil
Tel) 55-19-21065227, E-mail) rocharlesf@gmail.com

Imaging Science in Dentistry · pISSN 2233-7822 eISSN 2233-7830

of the most important factors that affect the prognosis and longevity of dental implants, as the progression of dehiscence defects may lead to gingival recession, bone loss, and consequently, dental implant failure.[1,4,5] Periapical radiography is a recommended imaging modality for evaluation and follow-up after dental implant placement.[6] However, periapical radiographs should not be requested to detect bone loss in the buccal and/or lingual cortical bone around a dental implant due to the inherent limitations of 2-dimensional images, such as the superimposition of anatomical structures and inability to depict the buccal-lingual level of bone tissues around the implant.[7] According to the current guidelines, cone-beam computed tomography (CBCT) is the first-choice examination for evaluating the detection of bone defects affecting the cortical plates around dental implants.[8,9] Nevertheless, there is still no consensus in the literature on the diagnostic efficacy of CBCT for the diagnosis of peri-implant dehiscence, due to the production of artifacts by high-density materials (e.g., titanium and Zr implants) that impair the diagnostic image quality of CBCT scans.[6,10,11]

The beam-hardening phenomenon is a major factor that reduces the quality of CBCT images when high-density materials such as titanium-zirconia (Ti-Zr) and Zr ($Z_{Ti} = 22$; $Z_{Zr} = 40$) are present in the dental arches. The regions near these high-density materials are impaired by hyperdense streaks and dark bands that overshadow the bone tissue around the dental implants.[12] Several factors may reduce the artifacts generated by high-density materials, ranging from physical factors inherent to the material used to manufacture dental implants to factors related to the acquisition parameters of CBCT images (milliamperage [mA] or kilovoltage- peak [kVp]), the number of basis images, and use of the metal artifact reduction (MAR) tool).[13-15] A previous study[12] showed that increasing the kVp level in combination with use of the MAR tool reduced the appearance of artifacts generated by different dental implants in regions near and far from the material that generates the artifacts. Considering that artifacts can impair the diagnosis of dehiscence on CBCT, an investigation of factors that could decrease artifact production, such as increasing kVp and using the MAR tool, is clinically relevant.

Thus, the purpose of the present study was to assess the influence of kVp and the MAR tool on detection of buccal and lingual dehiscence bone defects around Ti-Zr and Zr implants using CBCT images. The null hypothesis was that the kVp level and the MAR tool would not influence the diagnosis of dehiscence bone defects regardless of the cortical plate involved (buccal or lingual).

Materials and Methods

This study was approved by the local Research Ethics Committee (protocol number #24952219.0.0000.5418). The sample was composed of 3 dry edentulous human mandibles, which had alveolar bone edges with preserved height for the placement of dental implants in the posterior region.

Implant placement and simulation of dehiscence defects

First, a #1092 cylindrical drill (#1092, KG Sorensen, São Paulo, SP, Brazil) was used to prepare cylindrical holes in the left and right posterior regions of each mandible, with at least 1 mm between them, to allow the alternating fitting of 2 dental implants: a Ti-Zr implant (Straumann SLActive, Institute Straumann, Basel, Switzerland) and a Zr implant (PURE Ceramic, Institute Straumann, Basel, Switzerland), both measuring 3.3 × 8 mm. In total, 20 holes were prepared (1 mandible with 8 holes and the other 2 with 6 holes) (Fig. 1A).

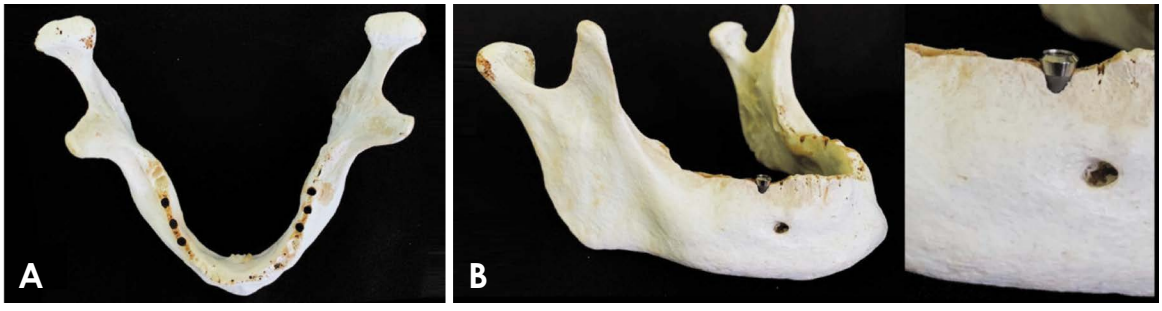

Fig. 1. A. Top view of a mandible used in the study shows the 6 holes prepared for the placement of the implants. B. A titanium-zirconia implant is positioned in 1 of the holes, in which a dehiscence defect was prepared in the buccal cortical (image with smaller and greater magnification).

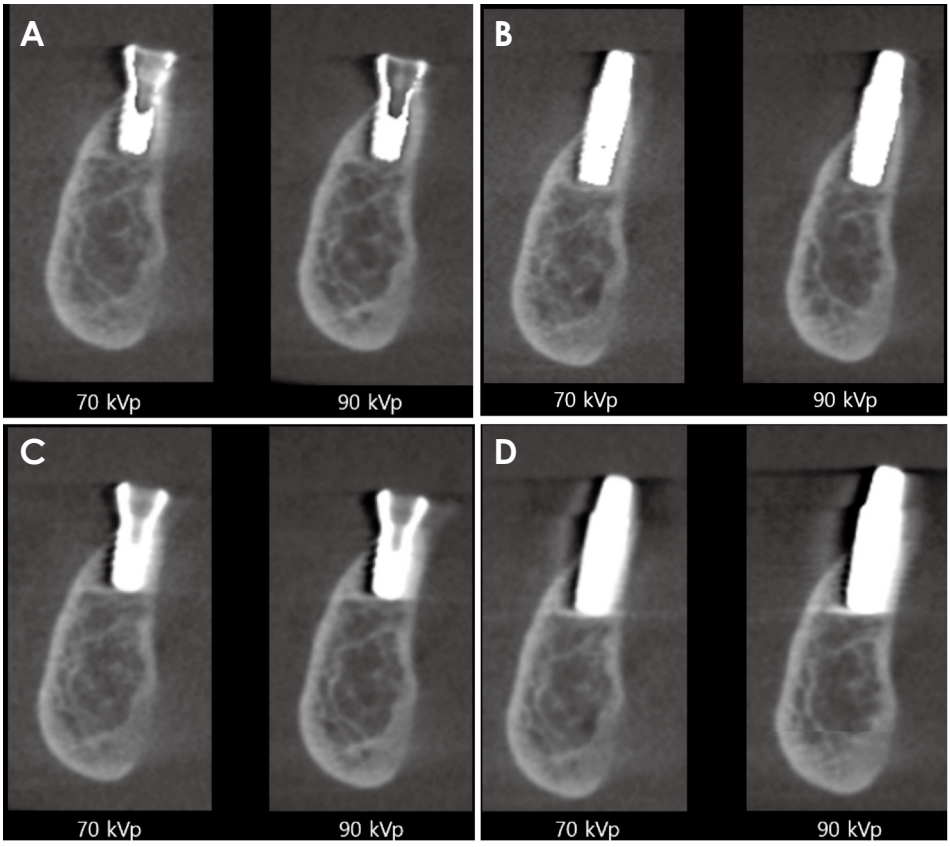

Fig. 2. Sagittal cone-beam computed tomographic reconstructions show the presence of dehiscence defects in the buccal cortical plate and the absence of bone defect (control cortical plate) in the lingual cortical plate according to the different factors tested (implant material, kVp, and metal artifact reduction condition). A and C: Titanium-zirconia implants, B and D. Zirconia implants.

Subsequently, the holes were randomly selected to create dehiscence defects in the buccal and/or lingual cortices of the mandible. For this, a trained dental surgeon carefully used a spherical drill (#1014; KG Sorensen, São Paulo, SP, Brazil) to create semi-circular dehiscence defects measuring 3 mm in height in the mandibular cortices (Fig. 1B). The thickness of the control cortices (without defects) was standardized using a caliper (Digimess, São Paulo, Brazil), and only those with remaining bone thickness between 1 and 2 mm were considered valid for the study. In 4 cases, the thickness of the control cortex exceeded the estimated size, so these cortical plates (2 buccal and 2 lingual) were excluded from the evaluations. Therefore, 19 dehiscence defects were performed (distributed between buccal and lingual cortical plates) and the remaining cortices constituted the control group (17 cortical plates).

CBCT image acquisition

Individually, each mandible was fixed by wax in a plastic container (16 cm diameter) filled with water to mimic the interactions of the X-ray beam with soft tissues, as occurs in clinical conditions.[12] The CBCT images were acquired using a Picasso Trio unit (Vatech, Hwaseong, Korea) for both groups of implants tested under 2 protocols with distinct energies of the X-ray beam: low energy (70 kVp) and high energy (90 kVp). The other acquisition parameters were fixed in 5 mA, a field of view (FOV) of 8 cm × 5 cm, and a voxel size of 0.2 mm. For each protocol, 2 sets of images were acquired with the MAR tool enabled or disabled (Fig. 2). For all scans, the phantom was centered in the FOV and the guidance lines of the CBCT machine aided in standardizing the position of the phantoms for acquisition.

CBCT assessment

A total of 160 CBCT scans (2 levels of kVp × 2 MAR conditions × 20 implant sites × 2 types of implant material) were assessed individually by 3 oral and maxillofacial radiologists with more than 5 years of experience in CBCT evaluation previously trained using a medical display (MDRC-2124, Barco NV, Courtray, Belgium). The scans were randomized, and the examiners were blinded regarding the factors investigated in the present study. The images were dynamically evaluated using the OnDemand 3D software (CyberMed, Seoul, Korea) under dim-light conditions in a silent room. The examiners were allowed to use the zoom tool and adjust brightness and contrast according to their visual needs. For each CBCT scan, the examiners assessed the buccal and lingual cortical plates around the implant

regarding the presence or absence of a dehiscence bone defect using a 5-point scale (1: absent, 2: probably absent, 3: uncertain, 4: probably present, 5: present). Thirty days after completing the evaluation, the examiners re-assessed randomly selected scans (30% of the sample) to test intra-examiner agreement.

Statistical analyses

The weighted-kappa test was used to assess intra- and inter-examiner agreement considering the categorical 5-point scale used to assess the images. The area under the receiver operating characteristic (ROC) curve, sensitivity, and specificity were calculated according to the study factors investigated (kVp level, cortical plate, type of implant material, and MAR use). These results were compared by multi-way analysis of variance with the post-hoc Tukey test. The level of significance (α) was set at 5% ($P<0.05$). The power was calculated to be 75%. All analyses were carried out using the SPSS version 24.0 (IMB Corp, Armonk, NY, USA), with the significance level set at 5%.

Results

Intra- and inter-examiner agreement ranged from slight (weighted kappa = 0.10 and 0.13, respectively) to substantial (weighted kappa = 0.64 and 0.69, respectively) (Table 1).

The results of the diagnostic values are shown in Tables 2-4. The values of the area under the ROC curve were not significantly affected by any of the studied factors ($P>0.05$) (Table 1). For 70 kVp and without MAR, the area under the ROC curve values ranged from 0.55 to 0.76 regardless of the type of implant and cortical plate. A similar pattern was observed when the highest kVp level was tested, in which the values ranged from 0.59 to 0.73. When the MAR tool was enabled, the values of the area under the ROC curve ranged from 0.64 to 0.78 for the 70 kVp condition and from 0.59 to 0.70 for the 90 kVp condition. Overall, these values of the area under the ROC curve are considered acceptable.[16]

In contrast, the sensitivity was statistically significantly affected by the type of implant used ($P<0.05$). As shown in Table 3, Zr implants showed greater sensitivity, ranging from 0.67 to 0.89, than Ti-Zr implants, which had sensitivity values ranging from 0.07 to 0.30. The kVp ($P=0.58$), cortical plate ($P=0.58$) and MAR ($P=0.78$) did not influence the results. When the MAR tool was disabled, the sensitivity values ranged from 0.22 to 0.78 and from 0.19 to 0.70 for 70 and 90 kVp, respectively, regardless of the type of implant and cortical plate. A similar pattern was observed when the MAR tool was enabled, with values ranging from 0.19 to 0.82 for 70 kVp and from 0.07 to 0.89 for 90 kVp.

The specificity was also statistically significantly affected by the type of implant used ($P<0.05$). As seen in Table 4, Zr implants showed lower specificity (ranging from 0.37 to 0.56) than Ti-Zr implants (ranging from 0.96 to 1.00). The kVp ($P=0.92$), cortical plate ($P=0.76$) and MAR ($P=0.54$) did not influence the results. When the MAR tool was disabled, the specificity values ranged from 0.37 to 1.00 and from 0.41 to 1.00 for 70 and 90 kVp, respectively, regardless of the type of implant and cortical plate. Similarly, when the MAR tool was enabled, the values ranged from 0.44 to 1.00 for 70 kVp and from 0.52 to 1.00 for 90 kVp.

Table 1. Intra- and inter-examiner agreement for the detection of dehiscence bone defects

Examiners	1	2	3
1	0.64	0.19	0.13
2		0.10	0.69
3			0.19

Table 2. Area under the receiver operating characteristic curve of titanium-zirconia (Ti-Zr) and zirconia (Zr) implants according to the studied factors

kVp	Cortical plate	Without MAR		With MAR	
		Ti-Zr	Zr	Ti-Zr	Zr
70	Buccal	0.76 ± 0.12	0.55 ± 0.06	0.64 ± 0.18	0.69 ± 0.15
	Lingual	0.73 ± 0.18	0.63 ± 0.16	0.78 ± 0.05	0.68 ± 0.22
90	Buccal	0.73 ± 0.16	0.63 ± 0.19	0.59 ± 0.08	0.64 ± 0.19
	Lingual	0.66 ± 0.17	0.59 ± 0.24	0.59 ± 0.12	0.70 ± 0.18

MAR: metal artifact reduction tool

Table 3. Sensitivity of titanium-zirconia (Ti-Zr) and zirconia (Zr) implants according to the studied factors

kVp	Cortical plate	Without MAR		With MAR	
		Ti-Zr	Zr*	Ti-Zr	Zr*
70	Buccal	0.26 ± 0.17	0.67 ± 0.39	0.19 ± 0.23	0.81 ± 0.32
	Lingual	0.22 ± 0.19	0.78 ± 0.22	0.30 ± 0.17	0.82 ± 0.13
90	Buccal	0.30 ± 0.23	0.70 ± 0.13	0.07 ± 0.13	0.74 ± 0.36
	Lingual	0.19 ± 0.23	0.70 ± 0.13	0.15 ± 0.26	0.89 ± 0.11

MAR: metal artifact reduction tool, *: $P < 0.05$ compared with Ti-Zr

Table 4. Specificity of titanium-zirconia (Ti-Zr) and zirconia (Zr) implants according to the studied factors

kVp	Cortical plate	Without MAR		With MAR	
		Ti-Zr*	Zr	Ti-Zr*	Zr
70	Buccal	0.96 ± 0.06	0.37 ± 0.46	0.96 ± 0.06	0.44 ± 0.48
	Lingual	1.00 ± 0.00	0.41 ± 0.42	1.00 ± 0.00	0.56 ± 0.40
90	Buccal	1.00 ± 0.00	0.41 ± 0.45	0.96 ± 0.06	0.52 ± 0.39
	Lingual	0.96 ± 0.06	0.41 ± 0.42	1.00 ± 0.00	0.52 ± 0.45

MAR: metal artifact reduction tool, *: $P < 0.05$ compared with Zr

Discussion

The determination of scanning protocols for obtaining CBCT examinations with greater image quality is essential in the evaluation of complications after dental implant placement, mainly in the presence of artifacts generated by high-density materials.[5,17] The present *ex vivo* study aimed to investigate the influence of kVp and the MAR tool on the detection of dehiscence bone defects located in buccal and/or lingual cortical plates around dental implants made from distinct materials. The authors' hypothesis was that both factors that have been proven to decrease artifact production, especially when working together, could improve dehiscence diagnosis. It was also hypothesized that could be a difference in the detection of the peri-implant dehiscence according to the cortical plate involved (i.e., the buccal or lingual cortical plate) because a previous study[18] objectively showed a difference in the production of artifacts according to the involved cortical plate, as the lingual cortical plate was the most affected when objectively assessed. Further, the MAR tool was effective in decreasing the artifacts only on the lingual cortical plate due to the greater presence of artifacts in this area. However, in the present study, none of these factors influenced dehiscence diagnosis.

Previous studies have investigated the influence of several scanning parameters on the detection of dehiscence defects using distinct *in vitro* models.[5,17,19,20] However, according to the authors' best knowledge, this is the first study that used human mandibles to investigate the influence of these CBCT parameters on the detection of dehiscence bone defects. Although kVp, MAR, and the cortical plate did not affect dehiscence detection, different behaviors were observed regarding diagnostic performance according to the material of the dental implant, as Zr implants showed greater sensitivity and lower specificity values than Ti-Zr implants for the detection of peri-implant dehiscence defects.

The type of implant material is a factor that may impair the image quality in areas close to the implant in CBCT images, as it is expected that implant materials with higher atomic numbers could lead to greater formation of metal artifacts from the beam-hardening phenomenon and the material volumetric distortion.[7,12,21] The present results showed that the presence of Zr implants ($Z_{Zr} = 40$) was associated with higher sensitivity values and lower specificity values than were observed for Ti-Zr implants ($Z_{Ti} = 22$). It was hypothesized that the higher expression of hyperdense streaks from the beam-hardening phenomenon and the increase of physical volume from the blooming effect may explain these findings. First, the expression of hyperdense streaks on cortical plates may have covered the cortical plates (healthy or with dehiscence). Additionally, as reported in the literature,[21] the artificially increased volume of the implant from the blooming effect may have caused an underestimation of the cortical thickness. Thus, both effects may

have contributed to the examiners more frequently assigning scores 4 and 5, which resulted in an increase in correct answers when there was dehiscence (increased sensitivity) and in incorrect answers when there was no dehiscence (decreased specificity).

The superior ability to diagnose bone defects around dental implants using CBCT images than using 2-dimensional radiography images is widely known;[22,23] however, the accuracy is still moderate, which makes further studies on CBCT protocols necessary.[19,24] There is still a lack of information or contradictions in the literature regarding the acquisition parameters that are most appropriate to obtain an image with higher diagnostic quality. Although it is known that peri-implant dehiscence defects are more often detected when CBCT images are acquired with a higher spatial resolution and with full-rotation of the machine, there was no information on the influence of kVp on this diagnostic task.[20] According to the current results, an increase from 70 to 90 kVp did not increase the detection rate of peri-implant dehiscence.

Several CBCT machines offer machine-specific MAR tools that work, in most cases, in the data reconstruction stage through the homogenization of gray values, especially in the regions where the artifacts are most strongly expressed. Their effectiveness has been widely proven when assessed objectively.[25] However, the effectiveness of MAR tools is less clear when subjectively assessed. Previous studies reported that MAR tools did not improve the diagnosis of vertical root fracture,[26] furcal perforation,[27] periodontal bone defects,[17] and peri-implant bone defects.[20] However, a recent *in vitro* study[5] evaluated the influence of the MAR tool of a different CBCT machine (Promax 3D Max; Planmeca Oy) combined with an image filter to noise optimization on the detection of peri-implant bone defects created in sheep jaws around 3 types of implants (titanium, Ti-Zr and Zr), and found better performance when those 2 tools were applied simultaneously on the CBCT images. However, no influence was observed on the diagnostic performance when only the MAR tool was applied. Corroborating these previous studies, the current investigation did not observe an influence of the MAR tool of the Picasso Trio CBCT machine on the diagnosis of peri-implant dehiscence around both tested implants, regardless of the kVp level tested.

The diagnosis of peri-implant dehiscence is a challenge, especially when defects are restricted to the cervical level of the dental implant.[20,28] Furthermore, the greater presence of artifacts on the cortical plates is another reason that makes this assessment difficult, once this region is closer to the artifact-generating area. In the present study, standardized dehiscence bone defects were created at the cervical level of the implant, representing the initial stage of bone loss. These reasons may explain why intra- and inter-examiner agreement ranged from poor to reasonable in the present results. Previous studies[5,20] reported low agreement values when the same diagnostic task was assessed using bone defects created on sheep jaws (0.30-070 and 0.20-0.63 for intra- and inter-examiner agreement, respectively) and bone ribs (0.40-0.47 for both types of agreement). However, these studies did not report the standardization of the control cortical plate thickness, as thicker cortical plates can be easily diagnosed. In contrast, the bone defects in the current investigation were created only at the cervical level of the implant, and the cortical plates were carefully selected to have a standardized thickness between 1 and 2 mm.

The current investigation is an *ex vivo* study that presents inherent limitations regarding the study design. However, it is important to highlight that this methodology is the only ethically acceptable way to assess various factors, such as the implant material, kVp level, and MAR tool, through CBCT scans. The main reasons why this methodology cannot be performed in a clinical scenario are the need to perform multiple CBCT scans and the biological risks inherent to ionizing radiation exposure to patients added to the lack of a gold standard. Furthermore, another limitation of the current study is that the bone defects were artificially made using spherical burs. Although using this type of burs made it possible to standardize the morphology and size of bone defects, this defect model may differ from those seen in the clinical setting regarding size, shape, and borders.

In conclusion, kVp and the MAR tool did not influence the diagnosis of dehiscence bone defects around dental implants, regardless of their buccal or lingual location. However, greater sensitivity and lower specificity values were observed in the presence of Zr implants than around Ti-Zr implants, regardless of the CBCT acquisition parameters tested.

Conflicts of Interest: None

References

1. Pinheiro LR, Scarfe WC, de Oliveira Sales MA, Gaia BF, Cortes AR, Gusmão Paraiso Cavalcanti M. Effectiveness of periapical radiography versus cone beam computed tomography with different kilovoltage settings in the detection of chemically created peri-implant bone defects: an in vitro study. Int J Oral Maxillofac Implants 2017; 32: 741-50.
2. Busenlechner D, Fürhauser R, Haas R, Watzek G, Mailath G,

Pommer B. Long-term implant success at the Academy for Oral Implantology: 8-year follow-up and risk factor analysis. J Periodontal Implant Sci 2014; 44: 102-8.
3. Hafezeqoran A, Koodaryan R. Effect of zirconia dental implant surfaces on bone integration: a systematic review and meta-analysis. Biomed Res Int 2017; 2017: 9246721.
4. Akheshteh V, Eskandarloo A, Saati S, Jamalpour MR, Mohammad Gholi Mezerji N. Efficacy of periapical radiography and three cone-beam computed tomography systems for detection of peri-implant dehiscence defects: an in- vitro study. J Biomed Phys Eng 2020; 10: 751-60.
5. Bayrak S, Orhan K, Kursun Çakmak ES, Görürgöz C, Odabaşı O, Yilmaz D, et al. Evaluation of a metal artifact reduction algorithm and an optimization filter in the estimation of peri-implant dehiscence defects by using cone beam computed tomography: an in-vitro study. Oral Surg Oral Med Oral Pathol Oral Radiol 2020; 130: 209-16.
6. Schriber M, Yeung AW, Suter VG, Buser D, Leung YY, Bornstein MM. Cone beam computed tomography artefacts around dental implants with different materials influencing the detection of peri-implant bone defects. Clin Oral Implants Res 2020; 31: 595-606.
7. Sancho-Puchades M, Hammerle CH, Benic GI. In vitro assessment of artifacts induced by titanium, titanium-zirconium and zirconium dioxide implants in cone-beam computed tomography. Clin Oral Implants Res 2015; 26: 1222-8.
8. Lang NP, Berglundh T, Working Group 4 of Seventh European Workshop on Periodontology. Periimplant diseases: where are we now? - Consensus of the Seventh European Workshop on Periodontology. J Clin Periodontol 2011; 11: 178-81.
9. Lindhe J, Meyle J, Group D of European Workshop on Periodontology. Peri-implant diseases: Consensus Report of the Sixth European Workshop on Periodontology. J Clin Periodontol 2008; 35: 282-5.
10. Pelekos G, Acharya A, Tonetti MS, Bornstein MM. Diagnostic performance of cone beam computed tomography in assessing peri-implant bone loss: a systematic review. Clin Oral Implants Res 2018; 29: 443-64.
11. Jacobs R, Salmon B, Codari M, Hassan B, Bornstein MM. Cone beam computed tomography in implant dentistry: recommendations for clinical use. BMC Oral Health 2018; 18: 88.
12. Fontenele RC, Nascimento EH, Vasconcelos TV, Noujeim M, Freitas DQ. Magnitude of cone beam CT image artifacts related to zirconium and titanium implants: impact on image quality. Dentomaxillofac Radiol 2018; 47: 20180021.
13. Vasconcelos TV, Bechara BB, McMahan CA, Freitas DQ, Noujeim M. Evaluation of artifacts generated by zirconium implants in cone-beam computed tomography images. Oral Surg Oral Med Oral Pathol Oral Radiol 2017; 123: 265-72.
14. Mancini AX, Santos MU, Gaêta-Araujo H, Tirapelli C, Pauwels R, Oliveira-Santos C. Artefacts at different distances from titanium and zirconia implants in cone-beam computed tomography: effect of tube current and metal artefact reduction. Clin Oral Investig 2021; 25: 5087-94.
15. Nascimento EH, Gaêta-Araujo H, Fontenele RC, Oliveira-Santos N, Oliveira-Santos C, Freitas DQ. Do the number of basis images and metal artifact reduction affect the production of artifacts near and far from zirconium dental implants in CBCT? Clin Oral Investig 2021; 25: 5281-91.
16. Mandrekar JN. Receiver operating characteristic curve in diagnostic test assessment. J Thorac Oncol 2010; 5: 1315-6.
17. Kamburoglu K, Kolsuz E, Murat S, Eren H, Yüksel S, Paksoy CS. Assessment of buccal marginal alveolar peri-implant and periodontal defects using a cone beam CT system with and without the application of metal artefact reduction mode. Dentomaxillofac Radiol 2013; 42: 20130176.
18. Nascimento EH, Fontenele RC, Santaella GM, Freitas DQ. Difference in the artefacts production and the performance of the metal artefact reduction (MAR) tool between the buccal and lingual cortical plates adjacent to zirconium dental implant. Dentomaxillofac Radiol 2019; 48: 20190058.
19. de-Azevedo-Vaz SL, Vasconcelos Kde F, Neves FS, Melo SL, Campos PS, Haiter-Neto F. Detection of periimplant fenestration and dehiscence with the use of two scan modes and the smallest voxel sizes of a cone-beam computed tomography device. Oral Surg Oral Med Oral Pathol Oral Radiol 2013; 115: 121-7.
20. de-Azevedo-Vaz SL, Peyneau PD, Ramirez-Sotelo LR, Vasconcelos Kde F, Campos PS, Haiter-Neto F. Efficacy of a cone beam computed tomography metal artifact reduction algorithm for the detection of peri-implant fenestrations and dehiscences. Oral Surg Oral Med Oral Pathol Oral Radiol 2016; 121: 550-6.
21. Vanderstuyft T, Tarce M, Sanaan B, Jacobs R, de Faria Vasconcelos K, Quirynen M. Inaccuracy of buccal bone thickness estimation on cone-beam CT due to implant blooming: an ex-vivo study. J Clin Periodontol 2019; 46: 1134-43.
22. Vadiati Saberi B, Khosravifard N, Ghandari F, Hadinezhad A. Detection of peri-implant bone defects using cone-beam computed tomography and digital periapical radiography with parallel and oblique projection. Imaging Sci Dent 2019; 49: 265-72.
23. Song D, Shujaat S, de Faria Vasconcelos K, Huang Y, Politis C, Lambrichts I, et al. Diagnostic accuracy of CBCT versus intraoral imaging for assessment of peri-implant bone defects. BMC Med Imaging 2021; 21: 23.
24. Carter JV, Pan J, Rai SN, Galandiuk S. ROC-ing along: evaluation and interpretation of receiver operating characteristic curves. Surgery 2016; 159: 1638-45.
25. Freitas DQ, Fontenele RC, Nascimento EH, Vasconcelos TV, Noujeim M. Influence of acquisition parameters on the magnitude of cone beam computed tomography artifacts. Dentomaxillofac Radiol 2018; 47: 20180151.
26. de Rezende Barbosa GL, Sousa Melo SL, Alencar PN, Nascimento MC, Almeida SM. Performance of an artefact reduction algorithm in the diagnosis of in vitro vertical root fracture in four different root filling conditions on CBCT images. Int Endod J 2016; 49: 500-8.
27. Kamburoğlu K, Yılmaz F, Yeta EN, Özen D. Assessment of furcal perforations in the vicinity of different root canal sealers using a cone beam computed tomography system with and without the application of artifact reduction mode: an ex vivo investigation on extracted human teeth. Oral Surg Oral Med Oral Pathol Oral Radiol 2016; 121: 657-65.
28. Chiapasco M, Zaniboni M. Clinical outcomes of GBR procedures to correct peri-implant dehiscences and fenestrations: a systematic review. Clin Oral Implants Res 2009; 20 Suppl 4:113-23.